

SYNTHESIS AND CHARACTERIZATION OF TIN-BORON PHOSPHIDE COMPOSITE MATERIAL PREPARED BY USING SOLID STATE METHOD**¹.Mrs. B. Rajitha* ².Dr. BalaSubramanyam .N**

Dept. of Physics, Sri Padmavati Mahila Visvavidyalayam, Tirupati, Andhra Pradesh.

Dept. of Mechanical Engineering, S.V University College of Engineering, Tirupati, Andhra Pradesh.

*Corresponding Author Email id: rajithasujitha1@gmail.com

ABSTRACT

Boron phosphide (BP) is a promising III-V compound semiconductor known for its exceptional thermal stability, high hardness, and semiconducting properties, making it suitable for high-performance electronic and optoelectronic applications. In this thesis, BP was synthesized using the solid-state reaction method, a simple and cost-effective approach that enables the formation of high-purity materials through direct elemental reaction. The synthesis process involved a series of steps, including precise weighing, grinding, heating in a tubular furnace, washing, drying, and sample collection.

Comprehensive characterization techniques were employed to analyze the structural, chemical, and morphological features of the synthesized BP. X-ray Diffraction (XRD) analysis confirmed the crystalline nature and phase formation of BP. Raman spectroscopy provided insights into the vibrational modes and purity of the material. FTIR spectroscopy identified the presence of characteristic B–P bonds and validated the chemical structure. Scanning Electron Microscopy (SEM) revealed the surface morphology and particle distribution, indicating a uniform microstructure.

The results confirm the successful synthesis of boron phosphide with desirable physical and chemical characteristics. This study highlights the potential of solid-state synthesis as an effective route for producing BP and provides a foundation for further research in material development for electronic and photonic applications.

INTRODUCTION

Materials are fundamental building blocks of the physical world. Everything we interact with — from natural elements like rocks and plants to human-made items like computers and buildings — is made of materials. With advances in science and technology, the concept of materials has evolved far beyond classical classifications like solids, liquids, and gases. Today, materials are often defined not only by their composition but also by their structure at the micro and nano-scale, as well as their behavior in different dimensions (2D, 3D, and 4D). This thesis aims to provide a comprehensive overview of materials and focus specifically on modern dimensional classifications

1.1 Materials and Their Functional properties

A material is any substance or matter used to make physical things. In science, materials are defined based on their structure, properties, and function. The study of materials involves physics, chemistry, biology, and engineering and is known as materials science

Materials can be characterized by their:

- Mechanical properties (strength, elasticity).

- Thermal properties (conductivity, expansion).
- Electrical properties (resistivity, conductivity).
- Optical properties (reflection, absorption).
- Magnetic properties.

With the advancement of nanotechnology, materials are now also classified by their dimensional structure at the atomic or molecular level. These are:

Zero-dimensional (0D): Nanoparticles.

One-dimensional (1D): Nanowires and nanotubes.

Two-dimensional (2D): Sheets like graphene.

Three-dimensional (3D): Bulk materials.

2.4 Synthesis Workflow of Boron Phosphide

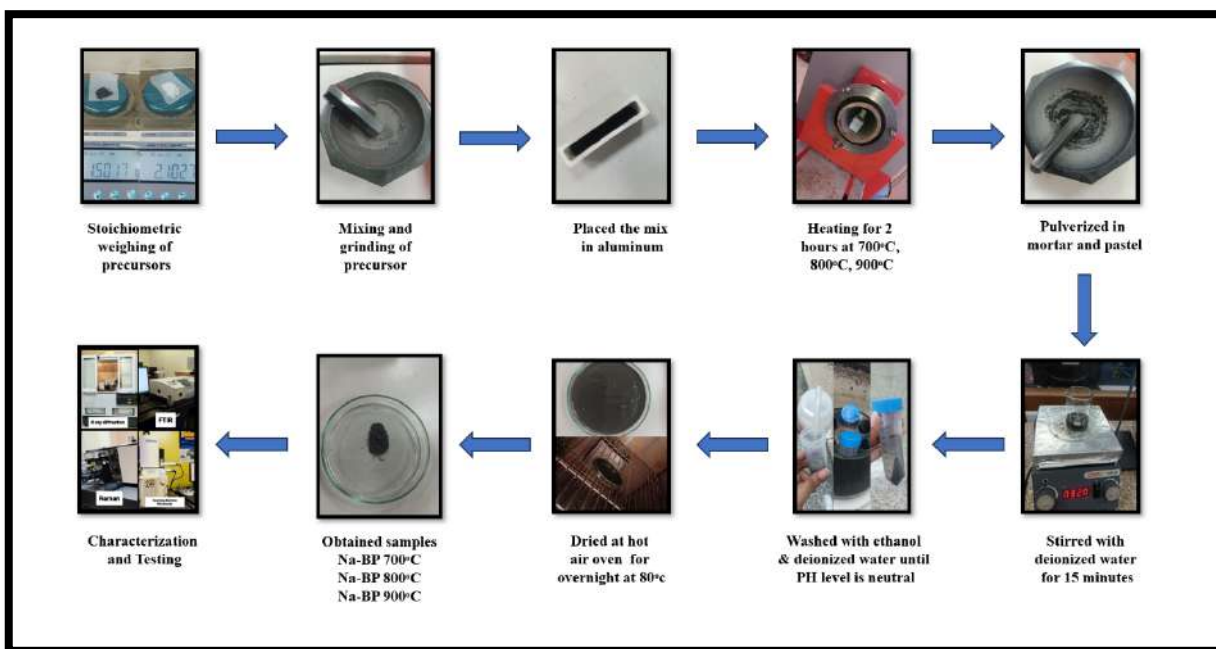


Fig 2.2 The Schematic diagram for synthesis of Boron Phosphide.

2.5 Fabrication and Design of Sn-Bp composite

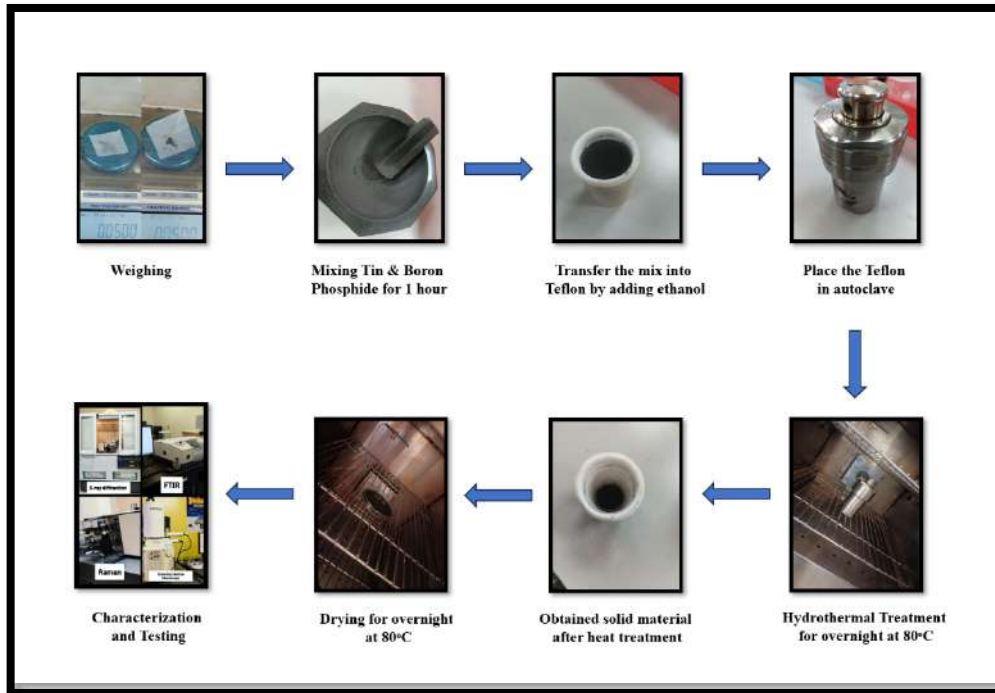


Fig 2.3 Schematic diagram for fabrication of Sn-BP composite

CHARACTERIZATION TECHNIQUES FOR BORON PHOSPHIDE

There are many types of spectroscopies, each suited for different applications. Some of the main types include:

- UV-Visible Spectroscopy.
- Infrared (IR) Spectroscopy.
- Raman Spectroscopy.
- Nuclear Magnetic Resonance (NMR) Spectroscopy.
- Mass Spectrometry (MS).
- X-ray Spectroscopy.
- Photoelectron Spectroscopy (PES).
- Atomic Absorption Spectroscopy (AAS).
- Atomic Emission Spectroscopy (AES).
- Electron Spin Resonance (ESR/EPR) Spectroscopy.
- Mössbauer Spectroscopy.
- Fourier Transform Infrared (FTIR) Spectroscopy.

Here we used X-ray Diffraction spectroscopy, Raman spectroscopy, and UV-visible spectroscopy .

1. X-Ray Diffraction

X-ray diffraction (XRD) is an analytical technique used to determine the structure of crystalline materials. When a beam of X-rays is directed at a crystal, it interacts with the atoms in the crystal lattice and is diffracted in specific directions. This diffraction occurs according to Bragg's law, which relates the wavelength of the X-rays to the spacing between atomic planes in the crystal. By measuring the angles and intensities of these diffracted beams, scientists can deduce the arrangement of atoms within the material. XRD is commonly used in materials science, chemistry, and geology to identify unknown compounds, determine crystal structures, and analyse phase composition. It is a non-destructive method, meaning the sample remains unchanged after analysis. XRD can be used on powdered or single-crystal samples and provides a unique diffraction pattern that acts like a fingerprint for each material, allowing for

Fig1: XRD Instrument.

precise identification and structural analysis . Instrumentation of XRD is illustrated in Fig 1.

2. Raman spectroscopy



Raman spectroscopy is a technique used to understand the composition and structure of materials by analysing how light interacts with them. When light hits a substance, most of it bounces back in the same



form, but a small portion of the light changes slightly due to interactions with the molecules in the material. This small change in the light's energy gives scientists information about the vibrations of the molecules, which are like tiny "fingerprints" that help identify what the material is made of. The process involves shining a laser light on the sample and measuring the scattered light with a special detector. The resulting data, called a Raman spectrum, shows peaks that correspond to different molecular bonds and structures.

Raman spectroscopy is a non-destructive method, meaning it doesn't damage the sample. Instrument of the Raman Spectroscopy is illustrated in Fig 2.

Fig 2: Raman spectroscopy instrument.

3. Fourier Transform Infrared(FTIR) Spectroscopy

Fourier Transform Infrared Spectroscopy (FTIR) is a powerful analytical technique used to identify and characterize organic, inorganic, and polymeric materials by measuring their infrared absorption spectra. FTIR works on the principle that molecular vibrations, such as stretching and bending of chemical bonds, absorb specific frequencies of infrared light. When a sample is exposed to a broad spectrum of infrared radiation, the molecules absorb energy at characteristic frequencies corresponding to their functional groups. These absorbed frequencies are recorded to generate an infrared spectrum, which serves as a molecular fingerprint of the material. The resulting FTIR spectrum displays transmittance or absorbance as a function of wavenumber (typically from 4000 to 400 cm^{-1}), enabling the identification of chemical bonds and functional groups present in the sample.

FTIR uses an interferometer, usually a Michelson interferometer, to collect all wavelengths of infrared light simultaneously. The collected data, known as an interferogram, is then mathematically transformed using Fourier Transform into a spectrum. This method offers several advantages over traditional dispersive IR spectroscopy, such as improved signal-to-noise ratio, faster data collection, and higher spectral resolution.

In materials science and chemistry, FTIR is widely used for qualitative and semi-quantitative analysis of solids, liquids, and gases. It helps determine the composition, detect impurities, monitor chemical reactions, and study structural changes in materials. In the context of nanomaterials or composites like boron phosphide or tin-doped systems, FTIR analysis helps confirm the presence of specific bonds (like B–P or Sn–O), verify the functionalization of surfaces, and assess interactions between components. The non-destructive nature and high sensitivity of FTIR make it a crucial tool for material characterization, aiding in the understanding of physicochemical properties and supporting the development of advanced



materials in various fields including energy storage, semiconductors, and biomedical applications . The image of Fourier Transform Infrared (FTIR) Spectroscopy is illustrated in Fig 3.

4. SCANNING ELECTRON MICROSCOPY

Scanning Electron Microscopy (SEM) is a powerful imaging technique that uses a focused beam of electrons to scan the surface of a sample. As the electrons interact with the sample, they produce signals that are detected and used to create detailed, high-resolution images of the sample's surface topography and composition. [Goldstein, J. I., et al., "Scanning Electron Microscopy and X-ray Microanalysis," 3rd Edition, Springer (2003). Instrument of SEM is illustrated in Fig 4.

Fig 4. Scanning Electron Microscopy Instrument.

5. EDX or EDS (Energy Dispersive X-Ray Spectroscopy)

Energy Dispersive X-ray Spectroscopy (EDX or EDS) is an analytical technique used to identify the



elemental composition of materials. Here's how it works in simple terms:

Fig 5 : EDX Instrument.

RESULT AND DISCUSSION

Several techniques were used to assess the generated Sn-BP Using the PANalytical X'Pert Powder instrument, which produces CuK-alpha radiation with an angular momentum of 1.540598 \AA , phase properties of the composite were determined. X-rays were collimated and focused on the sample. The range of 2θ Bragg-angles was 5° – 90° . Field Emission Scanning Electron Microscopy (FESEM) from Carl Zeiss, Model: Ultra-55 was utilised to examine morphology. The Oxford Instrument's Energy-dispersive X-ray spectroscopy (EDX)-model-INCAx-act was utilized to determine the element composition. Using Raman spectroscopy (LabRAM model-HR-800, HORIBA Jobin Yvon Ltd.) at a wavelength of (1000-3000) cm^{-1} , the quality of the produced Sn-BP was assessed. Every sample's optical properties were investigated using the FTIR Spectroscopy model, which has a wavelength range of 2,500–25,000 nm.

1. XRD Analysis

For structure properties BP was subjected to the XRD, Initially the boron phosphide is synthesis at different temperatures like 700°C , 800°C and 900°C . Here in fig 4.1.1a representing XRD pattern boron phosphide at various temperatures like 700°C , 800°C and 900°C . As the temperature increases the boron phosphide was evaluated as C-BP that means cubic-boron phosphide. Fig 4.1.1a clearly shows the effect of temperature on crystallinity and phase formation. At 700°C , the diffraction peaks are broad and of low intensity, indicating poor crystallinity and smaller grain size. As the temperature increases to 800°C , the peaks become sharper and more defined, suggesting improved crystal quality. At 900°C , the peaks are highly intense and sharp, confirming the formation of a well-crystallized BP phase. The observed diffraction peaks correspond to the cubic phase of BP without any noticeable impurity phases, indicating

| | | | | | |
|--|--|--|-----------------|--------------------|---------------------|
| | | | Phosphide phase | multiple 2θ values | Phosphide structure |
|--|--|--|-----------------|--------------------|---------------------|

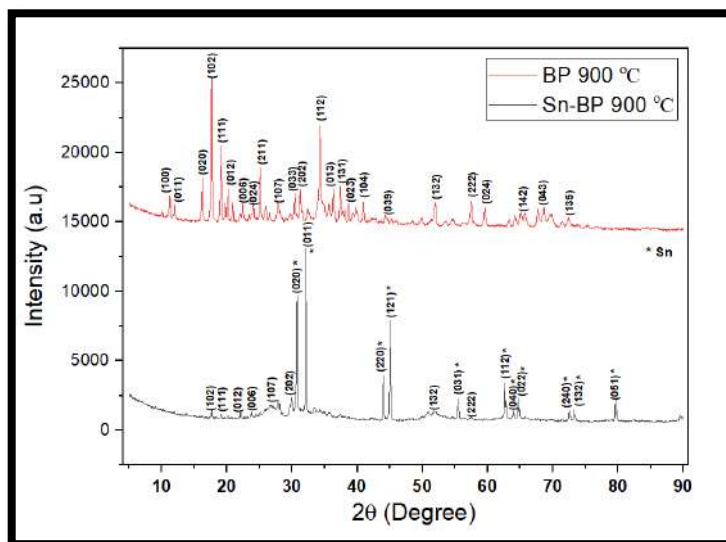


Fig 4.1.1b XRD for BP 900°C & Sn-BP 900°C

Table 2: XRD analysis of Boron Phosphide and Tin-Boron Phosphide at 900°C

| Parameter | Boron Phosphide (900°C) | Tin- Boron Phosphide (900°C) |
|-----------------------|---|---|
| Synthesis temperature | 900°C | 900°C |
| Phase formation | Single phase (Boron Phosphide) | Dual phase (Boron phosphide + Tin) |
| XRD peaks | Sharp peaks for Boron Phosphide (cubic structure) | Boron Phosphide peaks+ new Tin peaks and Sn-Boron Phosphide peaks |
| Crystallinity | High crystallinity (sharp and well-defined peaks) | Slightly lower crystallinity (Due to Sn addition) |
| Peak shift / change | Stable peak positions | Peak intensity of Boron Phosphide reduced new Sn peaks appeared |
| Interpretation | Pure Boron Phosphide synthesized | Tin successfully added forming Sn-BP composite |

2. RAMAN Spectra Analysis

Fig 4.1.2a displays the Tin-boron phosphide Raman spectra. Bands identified as D and G bands can be found in Raman spectra. The Raman spectroscopy analysis of BP and Sn-BP composites annealed at 900 °C reveals distinct structural characteristics influenced by Sn incorporation. The spectrum of pure BP (black line) shows sharp peaks at 474 cm⁻¹ and 818 cm⁻¹, corresponding to the characteristic vibrational

modes of crystalline boron phosphide. The presence of additional peaks at 1024 cm⁻¹ and 1064 cm⁻¹ further confirms the well-ordered crystal structure of BP. However, in the Sn-BP composite (red line), a significant broadening and suppression of these characteristic BP peaks is observed, indicating the distortion or disruption of the BP lattice due to Sn composite.

Fig 4.1.2a Raman of BP 900°C & Sn-BP 900°C

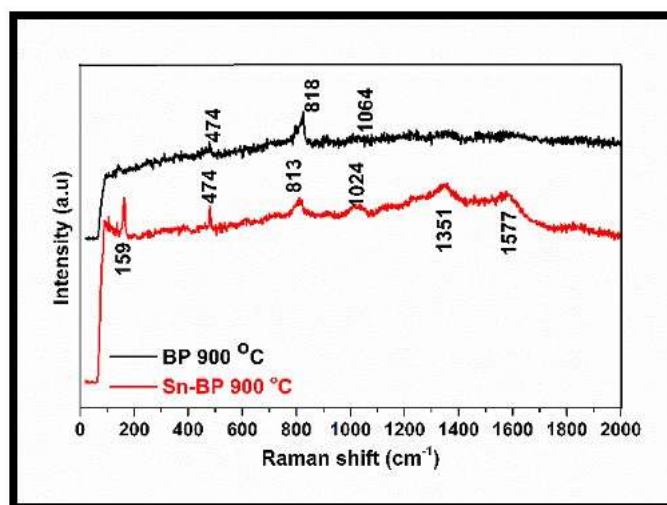


Table 3: Raman analysis of Boron Phosphide and Tin-Boron Phosphide at

| Sample | Raman shift (cm ⁻¹) | Peak assignment | Observation |
|-------------|---------------------------------|---|---|
| BP 900°C | 474 | B-P vibrational mode | Peak of Boron Phosphide |
| | 818 | B-P stretching vibration | Confirms BP structure |
| | 1064 | Possible B-B (or) P-P vibrations | Minor peak |
| Sn-BP 900°C | 159 | D-band (Defect-related) from Sn interaction | Indicates presence of defects (or) Sn composite |
| | 474 | B-P vibrational mode | Peak of Boron Phosphide |
| | 813 | B-P stretching vibration (weakly) | Peak slightly reduced due to Sn modification |
| | 1024 | Higher-order B-P mode (reduced intensity) | Indicates Sn interaction |
| | 1351 | D-Band (Defect mode of Sn induced) | More defects introduced |
| | 1577 | G-Band | Possible Sn phase |

New broad bands around 1351 cm^{-1} (D-band) and 1577 cm^{-1} (G-band) are evident, suggesting the formation of amorphous carbon or disordered graphitic-like structures. The peak at 159 cm^{-1} in Sn-BP may be attributed to tin-related vibrational modes. Overall, the Raman results suggest that tin incorporation leads to structural modifications, partial disorder, and the possible formation of Sn–C or Sn–P interactions, which alter the vibrational behaviour of the composite

4.3 FTIR Spectra Analysis

The FTIR spectrum of boron phosphide (BP) synthesized at 900°C is shown in Fig 4.1.2a. The spectrum reveals several characteristic absorption peaks, indicating the presence of various functional groups. A broad peak around 3430 cm^{-1} corresponds to O–H stretching vibrations, which may be due to surface-adsorbed moisture. The peak observed at 2926 cm^{-1} is attributed to C–H stretching, possibly from organic residues or contamination. A strong band at 2129 cm^{-1} is assigned to $\text{B}\equiv\text{N}$ or $\text{B}\equiv\text{C}$ triple bonds, which could be due to unreacted boron-containing species. The peak at 1635 cm^{-1} indicates the bending vibration of H–O–H, supporting the presence of absorbed water. The fingerprint region shows significant peaks at 1385 cm^{-1} , 1235 cm^{-1} , 1135 cm^{-1} , and 875 cm^{-1} , which are related to B–O, P–O, and B–P bonding vibrations. Notably, the peak around 712 cm^{-1} confirms the formation of B–P bonds, which is the characteristic vibrational mode for boron phosphide. These results confirm the successful synthesis of BP at high temperature and suggest the presence of some surface-bound groups and minor impurities.

The pure BP and Sn-doped BP (Sn-BP) synthesized at 900°C are shown in Fig 4.1.2b. Both samples exhibit similar absorption peaks, confirming the presence of common functional groups. The broad peak around 3430 cm^{-1} is due to O–H stretching, indicating moisture absorption on the surface. The peak at 2926 cm^{-1} corresponds to C–H stretching, possibly from residual organic compounds. A significant peak at 2129 cm^{-1} is observed, which may be associated with $\text{B}\equiv\text{C}$ or $\text{B}\equiv\text{N}$ bonds. In the Sn-BP sample, slight shifts and intensity changes are seen in the peaks, especially around 1635 cm^{-1} , 1385 cm^{-1} , 1235 cm^{-1} , and 875 cm^{-1} , suggesting interaction between Sn and the BP matrix. The characteristic B–P vibration is observed near 712 cm^{-1} , and a new or shifted peak around 629 cm^{-1} in the Sn-BP sample may indicate the

formation of Sn–O or Sn–P bonds. These changes confirm successful doping of Sn into the BP structure, slightly modifying its bonding environment [68][69].

Fig 4.1.2a FTIR of BP 900°C

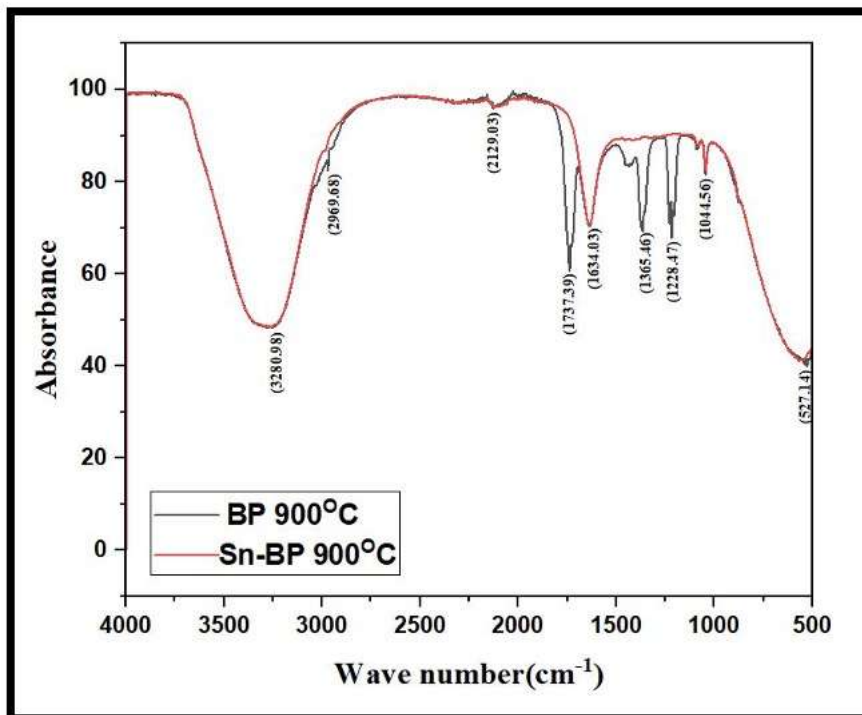
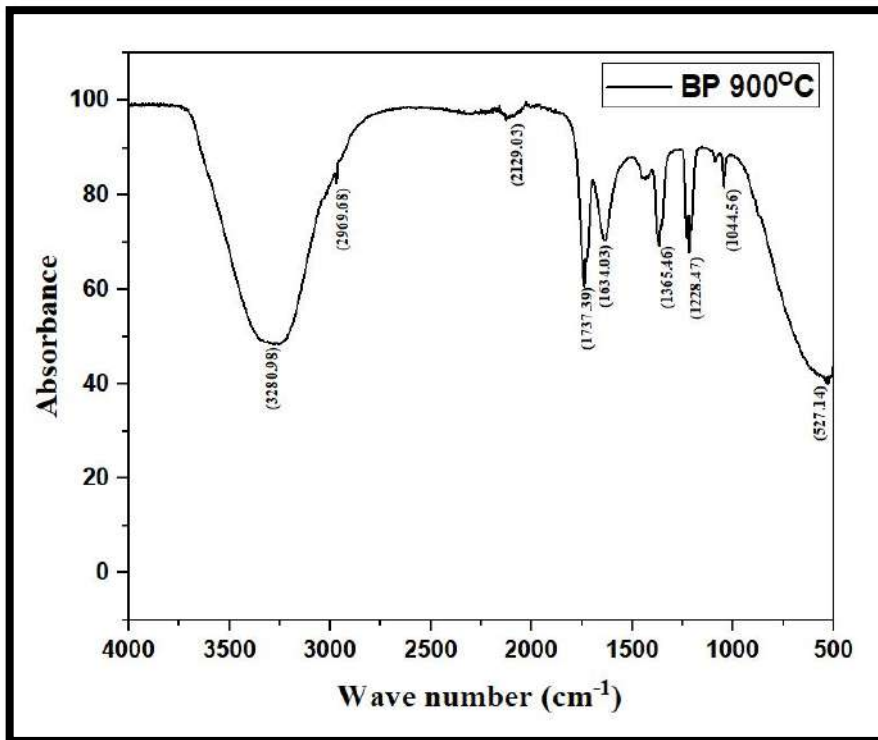


Fig 4.1.2b FTIR of Sn-BP 900°C

Table 4: FTIR analysis of Boron Phosphide and Tin-Boron Phosphide at 900°C

| Wavenumber (cm ⁻¹) | Peak assignment | Vibration type | Symmetric /Asymmetric | Observation |
|--------------------------------|------------------------------------|----------------------|-----------------------|---|
| 3280.98 | O-H stretching | Stretching | Broad/ Both possible | Due to moisture; observed in both Boron Phosphide Sn-BP |
| 2969.68 | C-H stretching | Stretching | Asymmetric | From organic; slightly shifted in Sn-BP |
| 2129.03 | CO ₂ (Or) impurity band | Stretching | Asymmetric | Weak band; may shift due to Sn presence |
| 1737.39 | Impurity band | Possibly stretching | Asymmetric | Minor peak; less sharp in Sn-BP |
| 1634.03 | B-O (or) P-O bending | Bending | Symmetric | Slightly reduced in Sn-BP |
| 1365.46 | B-O (or) C-H deformation | Bending/ Deformation | Symmetric | Observed in both; slightly more defined in Sn-BP |
| 1228.47 | P-O Stretching | Stretching | Asymmetric | Retained in Sn-BP |
| 1216.42 | P-O Stretching | Stretching | Symmetric | Main BP peak; slightly shifted (or) suppressed in Sn-BP |
| 1044.56 | B-P (or) P-O stretching | Stretching | Symmetric | Main BP peak; slightly shifted (or) suppressed in Sn-BP |
| 527.14 | B-P bond stretching | Stretching | Symmetric | Characteristic BP peak; present in both |

CONCLUSION

In this study, boron phosphide (BP) was successfully synthesized using the solid-state reaction method, demonstrating the viability of a cost-effective and scalable approach for compound formation. The synthesized material was thoroughly characterized through multiple analytical techniques, each confirming the structural and morphological integrity of BP. X-ray Diffraction (XRD) analysis revealed the crystalline nature of the synthesized BP, indicating phase purity and confirming the presence of a hexagonal or cubic structure based on diffraction peaks. Raman Spectroscopy supported the vibrational characteristics of BP, with distinct Raman modes aligning with literature values, further confirming the material's phase and bonding features. Fourier Transform Infrared (FTIR) Spectroscopy provided insight

into the bonding vibrations, highlighting the presence of B–P bonds and the absence of unwanted impurities, validating the chemical composition. Scanning Electron Microscopy (SEM) analysis revealed the surface morphology and particle size distribution, showing uniform microstructures suitable for potential electronic or optoelectronic applications.

REFERENCES

1. [Callister, W.D., & Rethwisch, D.G. (2020). *Materials Science and Engineering: An Introduction* (10th ed.). Wiley].
2. [Ashby, M., Shercliff, H., & Cebon, D. (2018). *Materials: Engineering, Science, Processing and Design* (4th ed.). Elsevier].
3. [Novoselov, K. S., et al. (2005). Two-dimensional atomic crystals. *Proceedings of the National Academy of Sciences*, 102(30), 10451–10453].
4. [Geim, A. K., & Novoselov, K. S. (2007). The rise of graphene. *Nature Materials*, 6(3), 183–191].
5. [Novoselov, K. S., Geim, A. K., et al. (2004). Electric field effect in atomically thin carbon films. *Science*, 306(5696), 666–669].
6. [Geim, A. K., & Novoselov, K. S. (2007). The rise of graphene. *Nature Materials*, 6(3), 183–191].
7. [Transition Metal Dichalcogenide, in subject area: *Material science from: progress in Crystal Growth and Characterization of Materials*, 2016. Vaskuri C.S. theja, Vellaisamy A.L. Roy].
8. [D.T. Debu, S.J. Bauman, D. French, H.O.H. Churchill, J.B. Herzog. Tuning infrared plasmon resonance of black phosphorene nanoribbon with a dielectric interface. *Scientific reports*, 8 (1) (2018), 10.1038/s41598-018-21365-2].
9. [Koski, K. J.; Cui, Y. The New Skinny in Two-Dimensional Nanomaterials. *ACS Nano* 2013, 7, 3739–3743, DOI: 10.1021/nn4022422].
10. [Electronic and transport property of two-dimensional boron phosphide sheets. Rajkumar Mondal, N. Bedamani Singh, Jyotirmoy Deb, Swarna Kamal Mukherjee, Utpal sarkar].
11. [Novoselov, K. S., et al. (2004). "Electric Field Effect in Atomically Thin Carbon Films." *Science*, 306(5696), 666–669].
12. [Geim, A. K., & Grigorieva, I. V. (2013). "Van der Waals heterostructures." *Nature*, 499, 419–425].
13. [Chhowalla, M., et al. (2013). "The chemistry of two-dimensional layered transition metal dichalcogenide nanosheets." *Nature Chemistry*, 5, 263–275].
14. [T. L. Chu, J. M. Jackson, and R. K. Smeltzer, *J. Cryst. Growth* 15, 254 (1972).
15. T. Nishinaga, H. Ogawa, H. Watanabe, and T. Arizumi, *J. Cryst. Growth* 13/14, 346 (1972)].
16. [Lipatov, A. N., Porechnaya, L. V., & Bushuev, N. N. (2001). Crystal structure and properties of boron phosphide. *Inorganic Materials*, 37(9), 899–902. <https://doi.org/10.1023/A:1012449006426>.
17. [Kang J.S., Wu H., Hu Y.J. Thermal properties and phonon spectral characterization of synthetic boron phosphide for high thermal conductivity applications. *Nano Lett.* 2017; 17:7507–7514].